From single droplet impact to micrometric droplet chains: scaling the effect of surface topography

A. S. Moita[1*], A. L. N. Moreira[1]
Instituto Superior Técnico – TU Lisbon, Portugal
anamoita@dem.ist.utl.pt and moreira@dem.ist.utl.pt

Abstract

Tuning the wettability based on surface structuring is becoming a hot topic, within the last years, due to several micro-scale applications. Many researchers consider an empirical trial-error approach, which may lead to contradictory and not always efficient results. In this context, the present work proceeds with the experimental identification of the topographical parameters which should lead to the optimum design of micro-patterns, to maximize the cooling performance of impinging droplets and streams. The surfaces made of silicon wafers are micro-textured with regular patterns of square pillars. The results show that for the patterns leading to homogeneous wetting, optimization of the parameter $r_f=(2l+\lambda_R)^2/[(2l+\lambda_R)^2+8lh]$was found to be a good path to design patterns leading to an improved cooling performance of the micro-textured surfaces in contact with both millimetric and micrometric droplet streams, within the nucleate boiling regime. Within the film boiling regime, the effect of the topography is clearly more evident. However, with the current surfaces we are on the limits of applicability of Wenzel's theory, so a further scaling down is required.

Introduction

Droplet/wall interactions have been widely explored within the last decade to develop smart interfaces and particularly enhanced surfaces to obtain an accurate control of heat and mass transfer, which is vital, for instance for cooling applications (*e.g.* [1]). Tuning the wettability based on surface structuring is becoming a hot topic, within the last years, due to several micro-scale applications. Many strategies have been recently explored to create custom made hydrophobic and/or hydrophilic surfaces applied to diverse situations, covering both micro and macro-scale systems (*e.g.* [2]). Among these, altering the surface wettability by changing its topography is probably one of the most recurrent approaches [3], probably due to its high ratio of simplicity *vs.* efficacy. In this context, "roughening" the surface has been argued for many years, as a good strategy to enhance heat transfer between liquids and solids, by increasing the liquid-solid contact area and therefore the convective heat transfer coefficients. However, recent studies [4] have shown that stochastic coatings are quite difficult to relate with the hydrodynamic phenomena, particularly when phase change is involved. Even when regular patterns are considered in the surface micro-structuring, an empirical trial-error approach is often followed exception made to few authors, *e.g.* [5]. Consequently, contradictory results can be found in the literature when reporting the effect of surface topography in the heat and momentum transfer phenomena. The crucial link that is missing is an accurate mapping of the wetting regimes, related to the heat transfer processes, using a systematic approach, as proposed, for instance by Moita *et al.* [6, 7]. The present work proceeds with the experimental identification of the topographical parameters which should lead to the optimum design, to maximize the cooling performance of impinging droplets and streams. Indeed, cooling of hot spots can be assessed based on single droplet impact, but in many cooling applications, the liquid delivery is made using one or various droplet chains, which alters significantly the boundary conditions of the problem. So, the study proposed here addresses a step by step approach to scale surface micro-structuring, from individual droplets on a dry surface to a wet condition. The scaling starts with millimetric droplets ($2.5<D_0<3.3$mm). Then, a small final sub-section will introduce the scaling down to micrometric droplets ($80\mu m<D_0<340\mu m$). The impact velocity is varied between $0.88<U_0<7 ms^{-1}$. The surfaces are made from silicon wafers and are micro-patterned using square and round structural elements, ranging from 5μm up to 200μm. Such wide range of the size of the structural elements is required for the accurate scaling, which depends on the size of the droplet and of the boundary conditions (*e.g.* dry *vs.* wet surface).

Experimental Methods

The experimental setup mainly consists on a droplet generator (Model MDG100) producing single droplets and monodisperse streams, which was directed onto a heated surface placed at a distance of 100mm. The test surfaces are coupled on a copper block heated by 264W cartridge heaters. The basic set-up is schematically repre-

* Corresponding author: anamoita@dem.ist.utl.pt

sented in Figure 1. To ensure stable impingement streams, while keeping the thickness of deposited liquid film under control, the droplet generator was used under very demanding working conditions, considering short duration impingement periods (ranging from a couple of milliseconds up to 1 second). Under these conditions it is difficult to keep the droplet stream always stable, so a reservoir was attached to a rotating disc, placed between the exit nozzle and the test surface, to displace the droplet stream when required (namely while it was unstable). The rotating disk is controlled by an electric motor, with variable velocity. Afterwards the disc is rotated and the stream can penetrate the orifice for a short time depending on the speed of the disc, thus impacting the test surfaces.

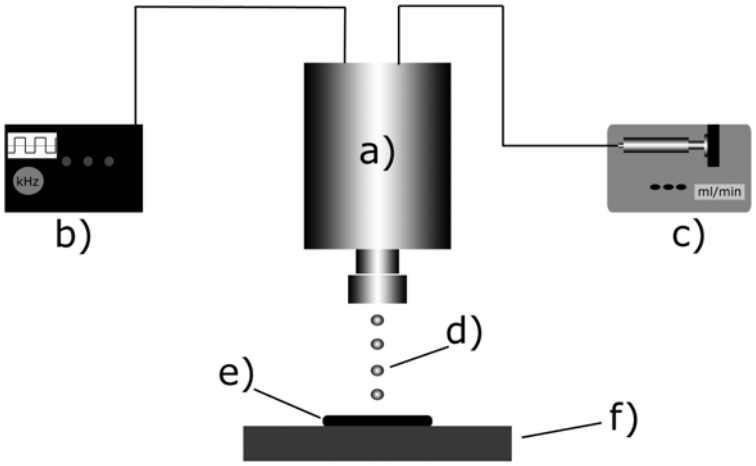

Figure 1 Display of the schematic of the experimental set-up: a) droplet generator, b) frequency generator, c)syringe pump, d) droplet stream, e) test surface, f) heating block.

The millimetric droplets are generated at a tip of a tube with 0.9mm of internal diameter. The micrometric droplets are produced using orifices ranging between 50 and 100μm. A jet is created by forcing the liquid through the orifice. This jet would naturally break up into drops of different sizes. However, if a disturbance in form of a square wave at the appropriate frequency is applied to the reservoir, the jet breaks up into uniform drops at the rate of one drop per excitation cycle, leading to a stream of equally spaced monosized droplets [8].

The excitation frequency was created using a Wavetek Model 191 frequency generator. Verification of the produced frequency was done with an oscilloscope to ensure that the settings corresponded to the correct frequencies.

Surface temperature of the targets is acquired using fast response thermocouples “Medtherm”. The thermocouples, with a response time of 50μs are 3mm apart, taking from the reference the thermocouple that is placed in the center of the droplet impact region (r=0mm). They are aligned with the top of the surface where the impact occurs. Another embedded thermocouple is used to control the cartridge heaters, using a PMA KS20-I controller.

The signal of the thermocouples is sampled with a National Instruments DAQ board associated with a BNC2120 and amplified with a gain of 300 before processing. Different acquisition frequencies were used to characterize the temporal variation of the instantaneous temperature. Hence, to capture the entire variation along droplet deformation process, a relatively low frequency must be used (of the order of 2Hz). Then to refine the measures to particular instants a larger frequency was considered, of the order of 10kHz.

Both an Image Acquisition System (IAS) and a Phase Doppler (PDA) System were used to characterize the impact dynamics and quantify the size and velocity of the droplets. The main element of the IAS is the high-speed camera (Phantom v4.2 from Vision Research Inc., with 512x512pixels@2100fps and a maximum frame rate of 90kfps). To record the impact history of the millimetric droplets, the frame rate was set to 2200fps. For the micrometric droplet streams the frame rate was increased up to 6300 fps (208 x 400 pixels). For the set-up used here, the resolution is 16μm/pixel.

The Phase Doppler instrument is a two-component system from Dantec. This system is composed by a covariance processor DANTEC 58N10 and a 300-400 mW air-cooled Argon Ion Laser from Spectra-Physics. The optical configuration of the two-component system is summarized in the Table 1.

The scattering angle of 70° was chosen because it was observed to reduce the sensitivity of the measurements to the refractive index to a minimum (Pitcher and Wigley [9]). Similar configurations were used by Cossali *et al.* [10] and Moita *et al.* [11] for the same reasons. The refractive indices are 1.334 for water and 1.359 for ethanol. The influence of the temperature on the refractive index was considered has in Moita and Moreira [11].

Table 1 Optical configuration of the phase Doppler instrument.

	Value
Transmitting optics	
Laser power [mW]	300
Wavelengths [nm]	514 and 488
Beam spacing [mm]	60
Transmitter focal length [mm]	310
Frequency shift [MHz]	40
Receiving optics	
Scattering angle [º]	70
Receiver focal length [mm]	310
Processor parameters	
U signal bandwidth [MHZ]	1.2
V signal bandwidth [MHZ]	0.4
S/N validation [dB]	0
Spherical validation [%]	10

Measurement procedure and working conditions

The size of the primary (and secondary) droplets larger than 200μm is mainly quantified based on high-speed visualization and image post-processing. For droplets smaller than 200μm both size and velocities were double checked by measurements with the Phase Doppler instrument.

To achieve a monodisperse droplet stream excitation frequency, flow rate and strobe light frequency were altered until a standing line of droplets appeared. Afterwards the uniformity of the generated droplet streams was verified with the PDA data. If the majority of the droplets was found to be constantly with a diameter tolerance (±10μm) the measurement was considered valid. Figure 2 exemplifies a measurement of a constant diameter around 140 μm.

The measurements are further compared to those determined from the relation $D_0 = 6Q \cdot (\pi \cdot f_e)^{-1/3}$, with D_0 as droplet diameter, Q as flow rate and f_e as the applied excitation frequency [8]. The agreement is fairly good in most of the cases. Larger disagreement is mainly attributed to instabilities of the stream. Only stable conditions were considered in the final measurements.

The working fluids are water and ethanol and were selected to allow exploring opposite wetting scenarios, which are known to strongly influence the thermal and hydrodynamic behaviour of the impacting droplets. The surface temperatures are varied over a wide range to cover all the heat transfer regimes, from film evaporation up to the film boiling. Table 2 summarizes the working conditions.

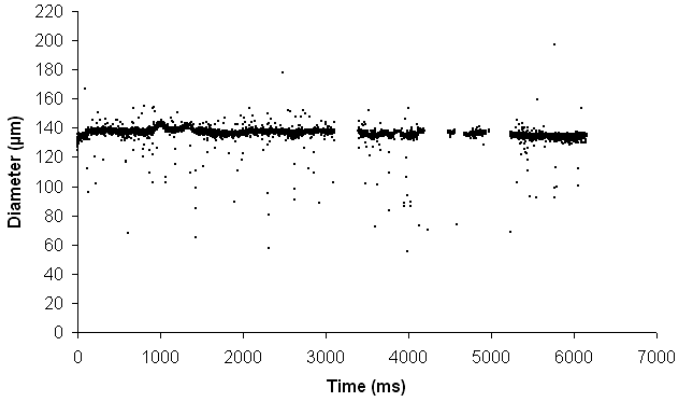

Figure 2 Example of a primary droplet stream measurement which was considered valid (30000 valid samples within 6 seconds, Q=0.8 ml/min f_e=8000 Hz. PDA measurements were performed at r=0mm, z=50mm from the surface).

Characterization of the test surfaces

The surfaces used here are made from a silicon wafer and are micro-patterned using square structural elements, ranging from 5μm up to 200μm. Such wide range of the size of the structural elements is required for the accurate scaling, which depends on the size of the droplet and of the boundary conditions (*e.g.* dry *vs* wet sur-

face). The size of the side is *l* and height *h*. The pillars are apart within a distance λ_R, as defined in Figure 3. The patterns are printed on the silicon wafer by lithography and processed by plasma etching. To reach higher pillars, the wafer surfaces were coated with aluminum, before the lithography. So, besides plasma etching, wet chemical etching is required for the aluminum coating. The micro-patterns are controlled to have known, precise values, using a profilemeter, with a measurement precision of 200Angstroms. An example of a roughness profile is depicted in Figure 3. Finally, the surfaces are checked by SEM/EDS analysis. Heterogeneity of the patterns was found to be lower than 3%. The wettability of the surfaces was also characterized, based on the static and dynamic contact angles, measured at room temperatures, inside a thermostatted ambient chamber (Ramé-Hart Inc., USA, model 100-07-00), using the Sessile Drop Method. An average value is considered for each pair liquid-surface which is determined from at least 8 measurements taken at different regions of the surface. The time evolution of the average contact angles is obtained by curve fitting and the final values are determined by extrapolation. The detailed measurement procedure has been described in previous works (*e.g.* Moita and Moreira [6]). The set of the surfaces used in this study is summarized in Table 3.

Table 2 Working conditions.

Milimetric droplets		
Liquid	**Water**	**Ethanol**
Primary droplet size - D_0 [mm]	3.1	2.6
Primary droplet velocity - U_0 [ms^{-1}]	1.4	1.4
Surface temperature – $T_{W,0}$ [ºC]	$T_{amb}< T_{W,0} <310$	$T_{amb}< T_{W,0} <260$
Micrometric droplets		
Liquid	**Water**	**Ethanol**
Primary droplet size - D_0 [μm]	$320<D_0<340$	$180<D_0<270$
Primary droplet velocity - U_0 [ms^{-1}]	$4.4<U_0<7.0$	$3.2<U_0<4.5$
Frequency - f_e[Hz]	$5000<f_e<9100$	$2100<f_e<5000$
Spacing - S [μm]	$180<S<580$	$940<S<1480$
Surface temperature – $T_{W,0}$ [ºC]	$T_{amb}< T_{W,0} <310$	$T_{amb}< T_{W,0} <260$

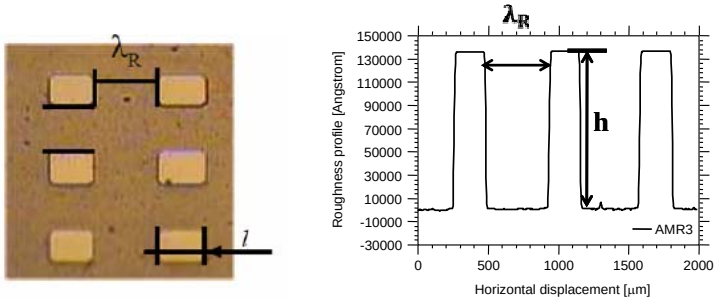

a) **b)**

Figure 3 a) Detail of a micro-structured surface, showing the definition of the dimensions *a*, *h*, and λ_R characterizing its topography. b) Sample 1-D roughness profile of the surface.

Wetting behaviour of the surfaces

The contact angles, measured with water on each tested surface are depicted in Table 3. These are mean values obtained from at least 8 measures taken at different regions of the surface. Complete wetting ($\theta_{eq}\approx 0º$) is observed for all the surfaces when wetted by the ethanol droplets. The establishment of different regimes and the applicability of the classical wetting theories of Cassie and Baxter and of Wenzel is still a very problematic issue, recently reviewed for instance in [12]. Also, for the current application, the contact angle is dependent of the velocity of the contact line. In this context, the authors recognize the need to establish wetting regimes based on real dynamic contact angles, which is still under development. However, most of the existing studies use "quasi-static" contact angles, which are basically static values [12]. In this context, the authors take the equilibrium contact angles as reference values and the description of the wetting behaviour using them is made with care, following an approach similar to that reported for instance in He *et al.* [13]. Based on this approach, which relates the roughness factor $r_f=f(h/l, \lambda_R/l)$ with the equilibrium angle to predict the wetting regime, following the classical approach of Wenzel and Cassie and Baxter, all the theoretical angles predicted by the Wenzel regime are significantly closer to those measured experimentally. According to Marmur [12] the relative size of the droplets in comparison to the characteristic size of the rough pillars is large enough to assure the applicability of the Wenzel and of the Cassie and Baxter's theory. Additionally, during the measurement of the contact angles, a visual inspection of the droplets in contact with the surfaces was performed with an optical microscope, coupled with a CCD camera, also seems to confirm the occurrence of a homogeneous wetting regime for all the surfaces at room temperature.

Table 3 Main topographical characteristics (defined in Figure 3) used in the customized micro-textured surfaces.

	l [µm]	h[µm]	λ_R [µm]	θ [º]
LISO	≈ 0	≈ 0	≈ 0	86.0
S1	60	1.2	212	68.2
S2	282	7.6	342	84.9
S3	224	13.5	446	66.8
S4	79	12.7	178	83.5
S5	105	23.7	405	44.9
S6	190	23.3	311	60.7
S7	190	23.5	116	65.1
S8	307	23.7	334	61.5
S9	46	23.4	158	74.4
S10	162	23.1	397	50.6
S11	290	23.3	338	70.0
S12	211	23.5	201	65.6
S13	43	23.8	53	57.2
S14	146	23.4	50	92.7
S15	76	23.2	104	65.3
S16	225	23.9	80	70.7
S17	152	23.4	77	56

Results and Discussion

In previous work a trend was proposed between the spreading diameter β(t) and the geometrical ratio h/λ_R, where h is the high of the rough pillars and λ_R is the distance between them. Under conditions of homogeneous wetting regime, the results suggested an increase of β(t) for higher values of h/λ_R. The impact velocity contributes to establish such regime. Consequently a similar trend was observed for the instantaneous temperature decay, which is attributed to the increase of the liquid-solid contact area and consequently to the increase of the convective heat transfer coefficient. This trend is valid for pillars with small cross sectional area ($l<<h$) but fails when a wider range of l is tested, covering values of the same order of magnitude of h and of λ_R. There is no consensual conclusion regarding the roughness parameters which should be considered either to predict the wetting regimes or to control the spreading diameter. Few authors as [16] argue that the pitch, λ_R should be considered. Others stand for the use of h/λ_R [14], while for instance [15] define the aspect ratio as l/λ_R. Under this scenario, a systematic study was performed to infer on the effect of each parameter, separately, in the spreading diameter and in the instantaneous temperature. The results depicted in Figure 4 show a major effect of increasing h and λ_R to increase the instantaneous spreading diameter and a minor, although non negligible effect of increasing the side of the pillar l. Hence the most unifying quantity gathering these three main parameters is the roughness ratio $r_f=(2l+\lambda_R)^2/[(2l+\lambda_R)^2+8lh]$. Figure 5a) shows a good trend of increasing of the spreading diameter with r_f: for homogeneous wetting regimes, increasing r_f is pinning the contact line, promoting the energy dissipation during the spreading phase. Naturally that the impact velocity affects the spreading velocity so it will contribute to increase the wetted area as well as the energy dissipation at the contact line, as it influences the dynamic contact angle. However, as shown in previous work, this is not the most relevant parameter for the impact conditions considered here. Consequently the recoiling process is much slower, so that overall wetted area is larger during the entire droplet-surface contact process. Consequently, more heat is removed from the surface. Thus, the decay of the instantaneous temperature is larger for increasing values of r_f (Figure 5b). This leads to an improved cooling performance confirmed by the larger heat flux, also for higher values of r_f, as shown in Figure 5c). The heat flux was determined based on the formulation of [17], which is not presented here due to paper length constrains. A similar trend is observed for the ethanol droplets, although in this case the complete wetting behaviour leads to a faster growth of β(t), which is much less sensitive to the effects introduced by surface topography. Hence, the difference between the curves is much less pronounced so that only three curves are shown here, to make the plot easier to read. Additionally, very small temperature decays are measured given the low values of the thermal properties of this liquid.

This trend is confirmed considering that all the patterns are leading to a homogeneous wetting regime which is the case, according to the aforementioned discussion on the **Wetting behaviour of the surfaces**. Also, representation of the contact angles as a function of these geometrical parameters, as performed in [13] and in [15] further confirms the homogeneous wetting regime.

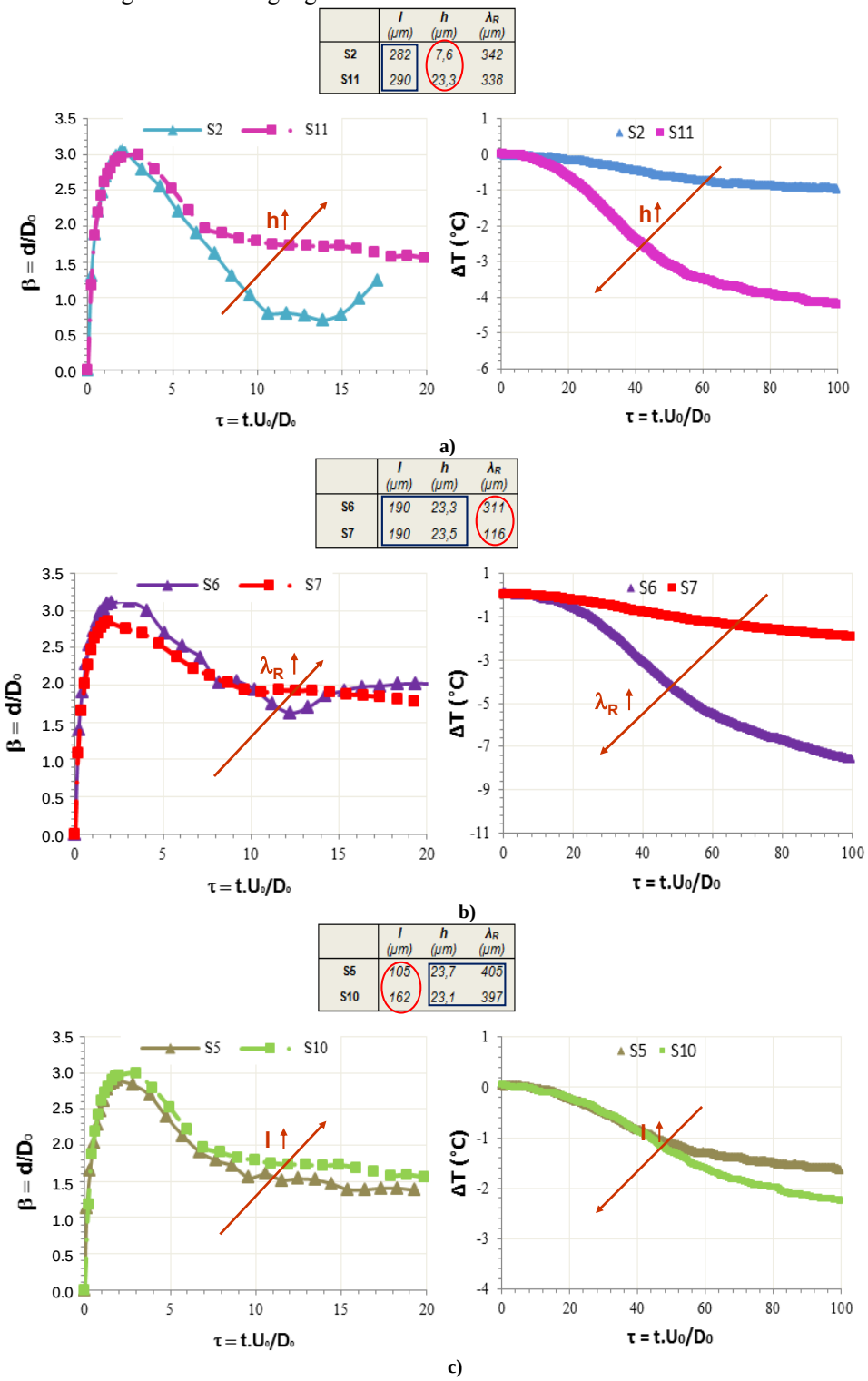

Figure 4 Effect of the geometric parameters characterizing the micro-textured patterns on the temporal evolution of the spreading diameter and on the instantaneous temperature: a) Effect of h, b) Effect λ_R, c) Effect of l. Water droplets (D_0=3.1mm, U_0=1.4ms^{-1}) impacting onto silicon wafer surfaces $T_{W,0}$=120ºC.

Deeper research is yet required to define the patterns leading to hydrophobic behaviour, using this approach of regular patterning. So, establishment of the transition regimes is not yet determined. Moreover, a detailed study of the dynamic angles and of the hysteresis over the contact line (which is out of the scope of this short

paper) is required to confirm the effect of the patterns with increasing r_f to promote energy dissipation. In fact this trend is not expected to be monotonic, as critical "large scale" roughness ratios were determined by Moita and Moreira [6] for which the trend was the opposite. So the turning value, which will dictate the transition criteria is now required to determine. While the control of the spreading diameter can be governed by the motion of the contact line, the effective increase of the contact area assured by the increasing of r_f will surely promote the heat transfer, so that even if the Wenzel theory, based on the contact areas is not always applicable, (although for the millimetric droplets analyzed up to now, the relative size of the droplets is sufficiently large to assure a good validation of Wenzel's theory [12]) the wettability will indirectly alter the contact area, thus affecting the heat transfer and the boiling mechanisms.

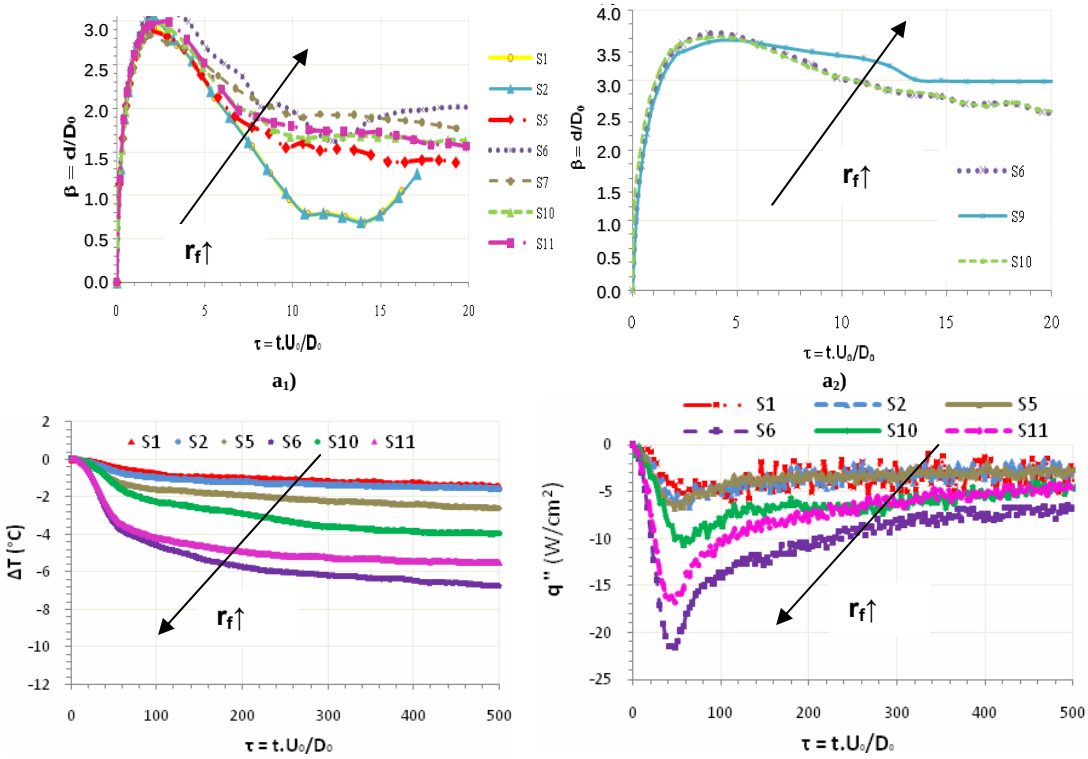

Surface	S1	S2	S5	S6	S9	S10	S11
r_f	1.005	1.021	1.053	1.074	1.1	1.058	1.064

Figure 5 Effect of the roughness ratio rf on the temporal evolution of the spreading diameter for a_1) water droplets (D_0=3.1mm, U_0=1.4ms^{-1}) and a_2) ethanol droplets (D_0=2.6mm, U_0=1.4ms^{-1}) impacting onto silicon wafers ($T_{W,0}$=120ºC) and consequent effect on b)the temperature decay and c)the heat flux.

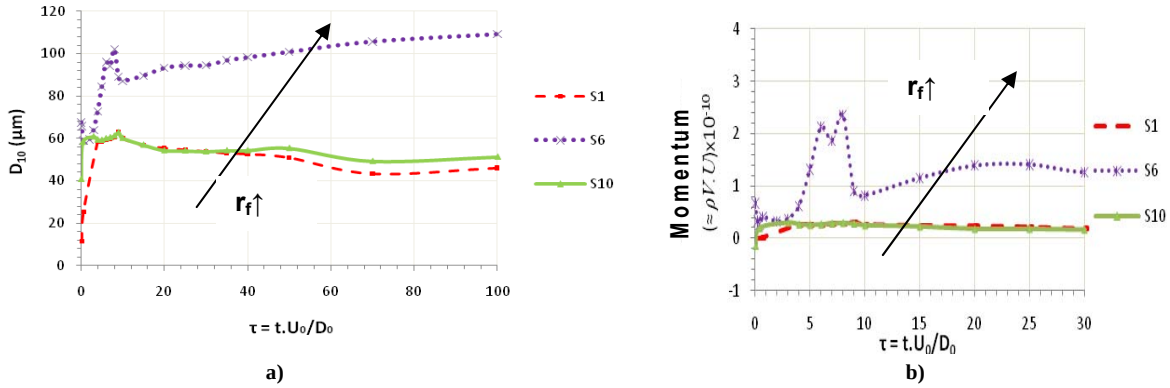

Figure 6 Effect of r_f on the thermal induced atomization a)D_{10}, b)Momentum of the ejected droplets. PDA measurements performed at r=0mm, z=2.5mm.

Moita and Moreira [6] argued that within the homogeneous regime, patterns promoting heat transfer would trigger the thermal induced atomization to occur earlier and give rise to droplets with larger sizes and higher ejecting momentum, as a result of the more intense boiling. This trend is confirmed, again as a function of r_f, in Figure 6, obtained with PDA measurements. For an ease of analysis, only 3 curves are shown, which are associ-

ated with patterns leading to significantly different values of r_f. Cleary, larger r_f, promoting heat transfer gives rise to larger secondary droplets, which are ejected from the lamella with higher momentum.

Scaling the patterns for micro-droplet streams

For impacts within the nucleate boiling regime, it was not possible to achieve stable streams for perfect droplet impacts onto dry targets. The deposited film is static, so the effect of the topography is less noticeable. However, within a first approximation, given that the secondary atomization is mainly thermally induced in the film, the effect of the surface roughness is still well defined by increasing values of r_f, which give rise to the earlier triggering of the thermal induced atomization, as a result of the increase of the contact area. This earlier triggering results in the deviation of the secondary droplets size distribution to smaller diameters (Figure 7a). On the other hand, within the film boiling regime (Figure 7b), the effect of the topography is clearly more evident. However, with the current surfaces we are on the limits of applicability of Wenzel's theory, so a scaling down is required. The large size of the elements act to promote dynamic disintegration which overcomes the thermal induced one, so that the rougher surface leads in fact to smaller secondary droplets. The scaling down of the new patterns will allow to deep the effect of r_f in the thermal induced behaviour within this regime.

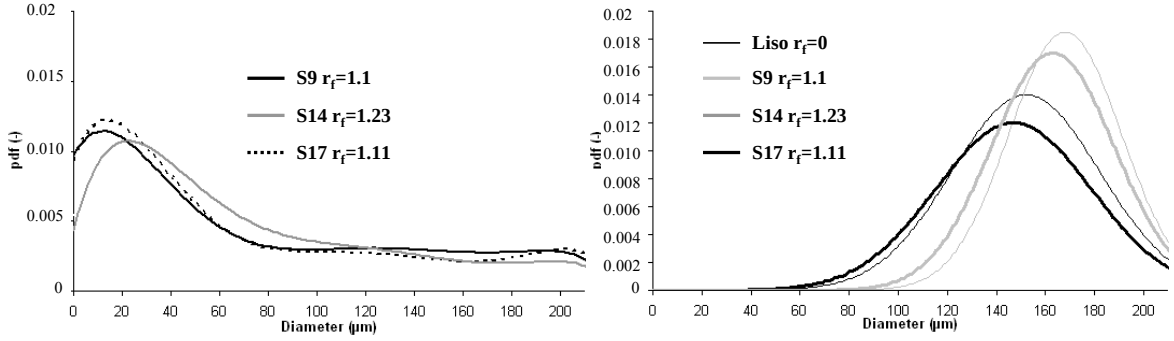

Figure 7 PDF of the secondary droplet size distribution resulting for impact of a monosize stream of ethanol droplets (D_0=180µm, u_0=3.2 m/s) over the micro-textured surfaces within: **a)** nucleate boiling regime ($T_{w,0}$=130°C) **b)** film boiling regime ($T_{W,0}$ =200°C). PDA measurements performed at r=1.2mm, z=1.2mm.

Summary and Conclusions

The present paper addresses the identification and scaling of the main geometrical parameters to be considered in the development of regular micro-patterns composed on square pillars. A systematic study was performed to infer on the weight of each of these parameters which established a dominating effect of the height of the pillars h and of the pitch λ_R, but a non negligible effect of the size of the side of the cross sectional area, l. Hence, for the patterns leading to homogeneous wetting, optimization of the parameter $r_f=(2l+\lambda_R)^2/[(2l+\lambda_R)^2+8lh]$was found to be a good path to design patterns leading to an improved cooling performance of the micro-textured surfaces in contact with both millimetric and micrometric droplet streams, within the nucleate boiling regime. Within the film boiling regime, the effect of the topography is clearly more evident. The large size of the elements acts to promote dynamic disintegration which overcomes the thermal induced one, so that the rougher surface leads in fact to smaller secondary droplets.

Acknowledgements

A. S. Moita is grateful to Fundação para a Ciência e a Tecnologia (FCT) for supporting her through the Post-Doc Fellowship (REF:SFRH/BPD/63788/2009).

References

[1] Weickgenannt, C. M., Roisman, I. V., Tropea, C., Yarin, A. L., *24th ILASS-Europe, Lisbon, Portugal* (2011).
[2] Ahn, H. S., Kim, M. H., *Nuclear Eng. And Tech.*, 43(3):205-216 (2011).
[3] Yeh, K.-Y., Cho, K.-H., Chen, L.-J., Langmuir2009, 25(24):14187-14194 (2009).
a. McHale, J. P., Garimella, S. V., *Int. J. Multiphase Flow*, 36:249-260 (2010).
[4] Gao, N., Yan, Y. Y., Chen, X. Y., Zheng, X. F., *Journal of Bionic Engineering,* 7 Suppl S59-S66 (2010).
[5] Moita, A. S., Moreira, Al. L. N., *Exp. Fluids*, 52:679:695 (2012).
[6] Moita, A.S., Tatta, M., Moreira, A. L. N., *24th ILASS-Europe, Lisbon, Portugal* (2011).
[7] Droplet Generator Manual of TSI MDG..
[9] Pitcher, G., Wigley, G., *Proc. 5th Int. Symp. Appl. Laser Tech. Fluid Mechanics*, Lisbon, Portugal, 1990, Edited by Adrian, R. J., Durão, D. F. G., Durst, F., Maeda, M., Whitelaw, J. H., Springer-Verlag Berlin, Heidelberg, Germany, 1991.
[10]Cossali, G. E., Marengo, M., Santini, M. *Exp. Thermal Fluid Sci.*, 29: 937-946 (2005).
[11]Moita, A. S., Moreira, A. L. N., *Experiments in Fluids*, 47:755-768 (2009).
[12]Marmur, A., *The European Phys. J. Special Topics*, 197:193-198 (2011).
[13] He, B., Neelesh, P. A., Lee, J., Languir2003, 19:4999-5003 (2003).
[14]Jung, Y., C., Bhushan, B., *Langmuir2009*, 25(24):14165-14173.
[15] Nakae, H., Yoshida, M., Yokota, M., *J. Mat. Sci.*, 40:2287-2293 (2005).
[16]Lee, J. B., Gwon, H. R., Lee, S. H., Cho, M., *Materials Trans.*, 51(9):1709-1711 (2010).
[17]Reichelt, L., Meingast, U., Renz, U., *Int. J. H. Mass Transf.*, 45:579-584.